High Resolution Difference Bands of Ethane C2H6 from torsionally Excited Lower States: Rotation-Torsion Structure of the $\nu 2$, $\nu 11$ and $\nu 4+\nu 11$ Vibrational States.

Carlo Di Lauro, Franca Lattanzi, Veli-Matti Horneman

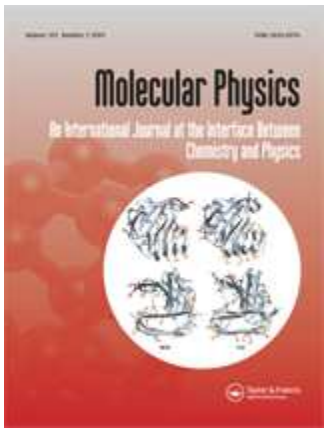

High Resolution Difference Bands of Ethane C2H6 from torsionally Excited Lower States: Rotation-Torsion Structure of the v2, v11 and v4+v11 Vibrational States.

Journal:	*Molecular Physics*
Manuscript ID:	TMPH-2011-0182.R1
Manuscript Type:	Full Paper
Date Submitted by the Author:	29-Jul-2011
Complete List of Authors:	di Lauro, Carlo; University of Naples, retired Lattanzi, Franca; University of Naples Federico II, Medicinal Chemistry Horneman, Veli-Matti; University of Oulu, Physics
Keywords:	high resolution infrared spectra, Infrared difference bands, Torsional splitting, Barrier to internal rotation, Torsional Coriolis coupling
Note: The following files were submitted by the author for peer review, but cannot be converted to PDF. You must view these files (e.g. movies) online.	
figures.zip	

High Resolution Difference Bands of Ethane C_2H_6 from torsionally Excited Lower States: Rotation-Torsion Structure of the ν_2, ν_{11} and $\nu_4+\nu_{11}$ Vibrational States.

Franca Lattanzi[a], Carlo di Lauro[a*], and Veli-Matti Horneman[b]

[a] Chimica Fisica, Università di Napoli Federico II, Via D. Montesano 49, I-80138 Napoli, Italy

[b] Departement of Physics, University of Oulu, Oulu, Finland

[*] Corresponding author: Carlo di Lauro, Via Bonito 27/C, I-80129 Napoli, Italy. car.dilauro@gmail.com

Abstract

A high resolution Fourier transform infrared spectrum of C_2H_6, measured with a pressure of 173.3 Pa and an optical path of 153.2 m, was analyzed between 1050 and 1295 cm^{-1}.

Extensive absorption due to the difference band ν_{11}-ν_4, and several rotation-torsion lines of the difference band ν_2-ν_4, in the region of the x,y-Coriolis resonance of ν_2 and ν_{11}, were observed.

This allowed us to perform a detailed rotation-torsion analysis of the upper states ν_{11} and ν_2.

The anomalous torsional structure, found in the non-degenerate vibrational state ν_2, can be explained as the effect of an Hamiltonian term accounting for a strong dependence of the torsional barrier height on the normal vibrational coordinate q_2. The value of the barrier height derivative $\frac{\partial V_3}{\partial q_2}$ is estimated to be 127±10 cm^{-1}.

We also could detect and assign "hot" difference transitions belonging to the $(\nu_4+\nu_{11})$-$2\nu_4$ band, yielding information on the upper state $\nu_4+\nu_{11}$. We believe that transitions from $3\nu_4$ to $2\nu_4+\nu_{11}$ are also detectable in the investigated region.

Keywords

High resolution infrared spectra. Infrared difference bands. Torsional splitting.
Barrier to internal rotation. Vibration-rotation Coriolis coupling. Torsional Coriolis coupling.

1. Introduction

Ethane is a key molecule owing to its highly symmetric geometry and peculiar internal rotation dynamics. It is also a relevant species in the applied research, because of its presence in the atmospheres of the Earth and outer planets, and in comets. For these reasons, the infrared active fundamental transitions of ethane have been extensively studied under high resolution, in spite of the particular complexity of the absorption spectrum, characterized by a high density of lines and anomalous rotation-torsion patterns generated by the interaction of several vibrational states, see Ref. [1-3] to mention only the most recent contributions. One may think that a detailed knowledge of the infrared inactive fundamental vibrational states is by far less important, but it is not so: In fact, infrared inactive modes ("g"-vibrational states under D_{3d}, the point group of the "rigid" staggered conformations) also occur in combination states that are involved in the complex interaction mechanisms affecting the observable absorption spectrum. Thus an accurate knowledge of the infrared inactive modes is quite helpful in the study of these complex mechanisms.

Owing to the selection rule u↔g holding for electric dipole transitions, g-fundamental vibrational states cannot be reached from the vibrational ground state (which is a g-state), but only from lower u-states, in the so called difference transitions. The lowest u-vibrational state of ethane is the first excited torsional state ν_4, about 289 cm^{-1} above the ground state, and this is the most favourable lower state for difference transitions, being the most populated u-state at the thermal equilibrium. Apart from the fact that the ν_4 state is less populated than the ground vibrational state, there is another factor that makes the difference transitions quite weak: they imply the change of two units (at the least) in the vibrational quantum numbers. Thus difference bands normally can be observed only in spectral regions free from stronger absorption,

The spectral region of ethane between the high-frequency wing of the fundamentals ν_9 (centered at 823 cm^{-1}) and the low-frequency wing of the fundamental ν_8 (centered at 1472 cm^{-1}), approximately between 1000 and 1300 cm^{-1}, is quite free from absorption and then it is a favourable region for the observation of difference bands. There are two g-vibrational fundamentals observable in this spectral region, as upper states in difference transitions from ν_4 : They are ν_2 (about 1397 cm^{-1}) with ν_2-ν_4 = ~ 1108 cm^{-1}, and ν_{11} (about 1468 cm^{-1}) with ν_{11}-ν_4 = ~ 1179 cm^{-1}.

Thus we decided to measure a high resolution Fourier transform infrared spectrum of ethane in the above spectral region, using a very long optical path, in the aim to measure and analyze the difference bands ν_2-ν_4 and ν_{11}-ν_4.

2. Experimental details

The experimental laboratory work was carried out in the Infrared laboratory at the University of Oulu with the BRUKER IFS 120 HR Fourier spectrometer. A C_2H_6 sample for laboratory use were obtained from Sigma-Aldrich. The studied weak absorption region from 940 to 1260 cm^{-1} required a very long recording time, 127 hours, with the sample at the pressure of 173 Pa in a multi-pass sample cell [4] with the absorption path length of 153.2 m. In the measurement the cell was provided with two potassium bromide (KBr) windows, a glowbar source was used, a germanium film on KBr was employed as a beam splitter and the infrared radiation was detected with a liquid nitrogen cooled mercury cadmium telluride (MCT) detector. The instrumental resolution due to the maximum optical path difference of the interferometer was 0.0016 cm^{-1}. The aperture broadening was 0.0018 cm^{-1} at 1100 cm^{-1} . Together with the Doppler broadening these instrumental effects gave the final spectral resolution 0.002 cm^{-1}, near the lower wavenumber end of the spectral region, and 0.0029 cm^{-1} near the higher end. All the spectra were calibrated using the transitions of carbonyl sulfide (OCS) in the $2\nu_2$ band. [5].

3. Description of the spectrum

The dominant extended feature observed in the investigated spectral region, between 1040 and 1295 cm^{-1}, is a perpendicular band that can be easily identified as the difference band ν_{11}-ν_4. In fact, the spacing of its Q-sub-branches is compatible with the value of the ζ-Coriolis constant expected for ν_{11}, and the differences of P, Q and R combinations sharing the same upper state correspond to the appropriate rotational energy differences in the ν_4 lower state. The *J*-structure of the Q-sub-branches degrades toward the high wavenumbers, because the *B*-rotational constant has a smaller value in the lower state, ν_4. The torsional splitting of the transition lines is of the order of 0.2 cm^{-1} as in ν_4, but with opposite sign, showing that ν_4 is the lower state and that the splitting in the upper state is considerably smaller. We could find and assign transitions of ν_{11}-ν_4 with $K''\Delta K$ from -17 to 14, denoting by K'' the absolute value of the quantum number associated with the total angular momentum component on the quantization axis, in the lower state. The $^rQ_3$ sub-branch, with its two torsional components, is shown in Fig. 1.

The density of the spectral lines becomes quite low far in the low-wavenumber wing, so that we could observe and identify very weak features, down to $K''\Delta K$ = -17. On the contrary, the line density remains high in the high-wavenumber wing, where the absorption due to the fundamentals ν_6 and ν_8 eventually starts. This is also due to the fact that "hot difference bands", mostly $(\nu_4+\nu_{11})-2\nu_4$ and $(2\nu_4+\nu_{11})-3\nu_4$, occur at higher wavenumbers than $\nu_{11}-\nu_4$, due to the large anharmonicity of the torsional mode ν_4. The fact that these "hot difference bands" are strong enough to be observed, can be understood by considering that the expressions for their transition probabilities, contain the square of the matrix element $\langle v_4, v_{11}=0 | (\partial^2\mu_\alpha / \partial q_{11}\partial q_4)_0 q_{11}q_4 | v_4 - 1, v_{11}=1\rangle$, with α = x or y, and then they are proportional to ν_4. Thus, assuming for ν_4, $2\nu_4$, and $3\nu_4$ the estimated anharmonic values 289, 545 and 757 cm^{-1}, from transition probabilities and lower level populations one finds that that the strengths of $\nu_{11}-\nu_4$, $(\nu_4+\nu_{11})-2\nu_4$ and $(2\nu_4+\nu_{11})-3\nu_4$ are in the ratios 1.00 : 0.58 : 0.31 at 296 K.

We were able to identify several sub-branches of $(\nu_4+\nu_{11})-2\nu_4$. They show a large torsional splitting, about 4 cm^{-1}, mostly due to the lower state. Fig. 2 shows the $^rQ_3$ sub-branch of $(\nu_4+\nu_{11})-2\nu_4$.

A few additional weaker Q-branches, which cannot be assigned to $\nu_{11}-\nu_4$ nor to $(\nu_4+\nu_{11})-2\nu_4$, are apparent at even higher wavenumbers. We believe that they belong to $(2\nu_4+\nu_{11})-3\nu_4$, on the basis of the intensity consideration of above.

The $\nu_2-\nu_4$ parallel band is very weak. Its Q-branch transitions occur as an irregular dense series of weak lines, between 1003 and 1007 cm^{-1}, but no line assignments could be done. However, several P-transition lines, activated by the x,y-Coriolis interaction of ν_2 and ν_{11} near resonance, could be detected and identified for K between 10 and 15. This will be discussed in the next paragraph.

4. The energy matrix and perturbations.

In the analysis of the spectrum we considered for the upper state the vibrational levels ν_2 (mainly symmetric CH_3 umbrella vibration of the two methyl groups, of A_{1s} symmetry under the extended molecular group G_{36}(EM), see Bunker and Jensen [6]) and ν_{11} (mainly degenerate symmetric CH_3 deformation of the two methyl groups, of E_{2d} symmetry under the extended molecular group G_{36}(EM)). These two states are coupled by an x,y-Coriolis interaction, like the

corresponding asymmetric modes ν_6 and ν_8 [2]. Later on we realized that an additional x,y-Coriolis interaction, between the states ν_{11} and $\nu_3+2\nu_4$, helped to improve the fit.

Small torsional splitting in a given vibrational state was accounted for as usual by the one-parameter expression [7, 8]

$$\nu^0(\vec{\nu}, \Gamma_t) = \nu^0 - 2(-1)^{v_4} X_v \cos(\sigma 2\pi/6) . \quad (1)$$

where $\vec{\nu}$ represents the ensemble of vibrational quantum numbers, inclusive of the torsional-vibration quantum number ν_4, X_v is a generally positive parameter whose value increases rapidly with ν_4, but depends also on the excitation of the small amplitude vibrational modes, and σ = 0, 1, 2, 3 for the components of torsional symmetries $\Gamma_t = A_{1s}$ (or A_{3s}), E_{3d}, E_{3s} and A_{3d} (or A_{1d}), using A_s and E_d vibrational basis functions. For larger splittings, a ν^0-value has to be determined for each of the four torsional components. Note that the components A_{1s} and A_{3d} occur with the even values of ν_4, whereas the components A_{3s} and A_{1d} occur with the odd values of ν_4. The torsional splitting in the ν_2 state is rather anomalous and we had to use four different values ν^0 for the the different torsional components A_{1s}, E_{3d}, E_{3s} and A_{3d},

Diagonal matrix elements were given as usual by

$$\begin{aligned} E[(\vec{\nu}, \Gamma_t, (\pm l), J, K] = \nu^0(\vec{\nu}, \Gamma_t) &+ (A-B)K^2 + BJ(J+1) \\ &- D_J J^2(J+1)^2 - D_{JK} J(J+1)K^2 - D_K K^4 \\ &\mp [2A\zeta - \eta_J J(J+1) - \eta_K K^2]K \end{aligned} \quad (2)$$

In the off-diagonal matrix elements, the torsional symmetries of interacting states depend on the specific states and on the shifts of quantum numbers. They can be determined following the procedures of Ref. [9].

The *l*-interaction with $\Delta k = \Delta l = \pm 2$, henceforth referred to as *l*(2,2), was taken into account within the state ν_{11}, with matrix elements

$$\left\langle \vec{\nu}_s, \Gamma_t, l = \pm 1, J, k \pm 1 \middle| \boldsymbol{H} \middle| \vec{\nu}_s \Gamma_t, l = \mp 1, J, k \mp 1 \right\rangle$$

$$-2(F + k^2 F_K)\{[J(J+1) - k(k+1)][J(J+1) - k(k-1)]\}^{1/2} \quad (3)$$

The x,y-Coriolis interaction was considered in the vibrational pairs ν_2 and ν_{11} and $\nu_3+2\nu_4$ and ν_{11}, with matrix elements

$$\left\langle \tilde{\nu}_s,\ \Gamma_t,\ l=\pm 1,\ J,k\pm 1 \left| \boldsymbol{H} \right| \tilde{\nu}_r,\ \Gamma_t, l=0, J, k \right\rangle =$$

$$\pm 2^{1/2}\,[Z_{r,s}+ Z_{r,sJ}\,J(J+1)][J(J+1)-k(k\pm 1)]^{1/2} \qquad (4)$$

The *l*-type interactions with $\Delta l = \pm 2$ and $\Delta k = \mp 1$, henceforth referred to as *l*(2,-1), within the state ν_{11} occurs with matrix elements

$$\left\langle \nu_{11},\ \Gamma_t,\ l=\pm 1,\ J,k \left| \boldsymbol{H} \right| \nu_{11},\ \Gamma_t \times A_{3d}, l=\mp 1, J, k\pm 1 \right\rangle =$$

$$(E+k^2E_K)\ (2k+1)\ [J(J+1)-k(k\pm 1)]^{1/2} \qquad (5)$$

Fig. 3 shows the Coriolis interactions of ν_{11} with the parallel vibrational states ν_2 and $\nu_3+2\nu_4$, in the region of the resonance. We could detect and assign P-transitions from ν_4 to ν_2, enhanced by the mixing of ν_2 and the (-*l*)-side of ν_{11}, in the region near the resonance (*K* from 10 to 15), see Fig. 4. For *K* equal to 12 and 13 both stronger and weaker transitions to the split torsional components of ν_2 were observed.

Fig. 3 also shows that the levels of ν_{11} which can be coupled by an interaction with $\Delta l=\pm 2$ and $\Delta k = \mp 1$ (*l*(2,-1) coupling) are always rather close to each other. Their energy separation is also influenced by the effect of the concomitant x,y-Coriolis interactions.

Some peculiar effects on the spectrum of these Coriolis perturbations are opposite to those described by di Lauro and Mills [10], because of the asymmetry of the lower vibrational state ν_4 with respect to a reflection through a plane $\boldsymbol{\sigma}_{xz}$ containing the molecular z-axis, and its bearing on selection rules. In fact, if we denote by ± the symmetrized vibration-rotation functions defined as

$$\left|\pm\right\rangle = \left(\left|K,l\right\rangle \pm \left|-K,-l\right\rangle\right)/\sqrt{2}\,, \qquad (6)$$

the vibration-rotation electric dipole selection rules (asymmetric↔symmetric with respect to $\boldsymbol{\sigma}_{xz}$) are +↔- for Q-transitions and ±↔± for P and R-transitions, contrary to what would hold for transitions from a symmetric lower state. As a consequence of this, the above x,y-Coriolis

interactions have no effect on the $^{r}R_0$ and $^{r}P_0$ sub-branches of ν_{11} and a larger effect than elsewhere (by a factor $\sqrt{2}$ in the matrix elements) on the sub-branch $^{r}Q_0$, see also Ref. [2].

Fig. 5 shows the *l*-type interaction mechanisms acting within the ν_{11} state. The $l(2,2)$ interaction ($\Delta k=\Delta l=\pm 2$) is always resonant for the $l=k=\pm 1$ pair, causing its splitting into the symmetrized combinations as in Equation (6). This splitting is transmitted to the $l=\mp 1$, $k=\pm 2$ pair by the $l(2,-1)$ interaction ($\Delta l=\pm 2$, $\Delta k=\mp 1$), with the coupling selection rule +↔-. Thus the transition lines with $K''\Delta K=-3$, ending to the above levels, appear each with four components, owing to the simultaneous effects of torsional and *K*-splitting, see the $^{p}Q_3$-transitions in Fig. 6.

This interaction mechanism and the *K*-doubling of the $K''\Delta K=-3$ levels in ν_{11} is quite similar to what has been observed in ν_8, see Ref. [2]. However the effects on the spectrum are different, because in the present case the lower state is ν_4 (asymmetric with respect to the reflection through the mentioned symmetry plane $\boldsymbol{\sigma}_{xz}$) instead of the ground state. In fact, in the present case the selection rules in the + and – labels are ±↔± for transitions with even $\Delta K+\Delta J$, and +↔- for transitions with odd $\Delta K+\Delta J$, contrary to what holds for the ν_8 fundamental. The details are discussed in the Appendix of Ref. [2].

The $l(2,2)$-splitting in the $l=k=\pm 1$ pair increases with *J*, and eventually its – component crosses the + component with $k=\pm 2$ coupled to it by the $l(2,-1)$ interaction, inverting the sign of the level displacements, see Fig. 5. This happens at $J=15$, and the most evident effect is a sudden change of the *J*-spacing from $J=14$ to $J=15$ (an increase of the spacing in the $^{r}Q_0$ sub-branch, and a decrease in the K+ components of $^{p}Q_3$, see Fig. 6). Because of the effect of this crossing, K+ is higher than K- up to $K=14$ included, and then becomes lower, This can be easily checked in Fig, 6, because the K+ transitions are stronger for odd *J* and the K- transitions for even *J*, for each torsional symmetry.

The effect of the *J*-crossing between 14 and 15 is also detectable in the sub-branch $^{r}Q_0$, where the displacements of the levels with $J=14$ and 15 are obviously opposite to those observed in $^{p}Q_3$, see Fig. 7. The strong level mixing near resonance can activate transitions with $\Delta K=\pm 2$, an in fact we could observe three $^{s}Q_0$ transitions ($\Delta K=2$), at $J=14$ (for the stronger torsional component) and $J=15$ (for both torsional components), also shown in Fig. 7.

5. Analysis and results.

The body of data processed in an iterative least squares calculation, according to the Hamiltonian model of the previous paragraph, consisted of wavenumbers corresponding to 1386 different

rotation-torsion upper states belonging to the ν_{11} and ν_2 vibrational states. Namely, we used 1277 wavenumbers of the ν_{11}-ν_4 transition (^{p}P-transitions for $K''\Delta K$ from -1 to -17, ^{r}R-transitions for $K''\Delta K$ from 0 to 14, $^{r}Q_0$ transitions, and three $^{s}Q_0$ transitions, with a maximum J-value of 37) and 109 wawenumbers of the ν_2-ν_4 transition (^{q}P-transitions activated by the x,y-Coriolis resonance of ν_2 with ν_{11}, for K from 10 to 15 and a maximum J-value of 28). As mentioned, we considered also the state $\nu_3+2\nu_4$, as a Coriolis perturber of ν_{11}. The account for an anharmonic interaction of ν_2 and $\nu_3+2\nu_4$ did not improve the fit, and this interaction was disregarded. Eventually the iterative calculations converged to a root mean square (RMS) deviation of 2.52×10^{-3} cm^{-1}, with the parameter values reported in Table 1.

Due to the lack of data relative to $\nu_3+2\nu_4$, we could determine only the values of ν°, X, A and B for this vibrational state.

The ν_{11} state

The values of the parameters for this state (mainly symmetric deformation of the two methyl groups) are rather similar to those found for ν_8 (mainly asymmetric deformation of the two methyl groups) in Ref. [2]. This holds also for the l-type interaction parameters (F and E), and in fact these interactions are quite important in both vibrational states. However, the infrared active fundamental band ν_8 appears much more complex than the difference band ν_{11}-ν_4, because of the effect of the combination state $\nu_4+\nu_{12}$ occurring quite close to ν_8. Also in ν_{11} the torsional splitting is considerably smaller than in non-degenerate states in the torsional lowest state (X=0.00110 cm^{-1}, against the ground state value of 0.00189 cm^{-1}) as expected from theory, see [11] and references therein. The x,y Coriolis interaction between ν_{11} and ν_2 is quite similar to that between ν_8 and ν_6 (ν_2 and ν_6 are mostly symmetric and asymmetric umbrella vibrations of the two methyl groups). The mechanisms generating the K-doubling of the levels $k=\pm2$, $l=\mp1$ in ν_{11} and ν_8 [2] are quite similar: In ν_{11} too the splitting can be accounted for by the combined effect of the $l(2,2)$ and $l(2,-1)$ interactions, as already discussed, without considering an effective direct interaction ($\Delta K=\pm4$, $\Delta l=\mp2$) within the vibration-rotation components of the doublet.

The values of the parameters of ν_{11} determined by Fernández and Montero from the Raman spectrum [12] (ν^0=1468.4, A=2.6575, B=0.6666, $A\zeta$= -0.8886, all in cm^{-1}), are in reasonable agreement with ours.

The ν_2 state

Although the observation of transitions to the ν_2 state is limited to the *K*-range between 10 and 15, near the Coriolis resonance with ν_{11}, the parameters of the ν_2 state could be determined quite well. In fact, it is worth to note that the body of observed ^pP-transitions to ν_{11} brings information on ν_2 even beyond the mentioned *K*-range, because of the interaction of the two states.

The torsional splitting of ν_2 is rather complex, and cannot be accounted for by the simple one-parameter expression of Equation (1). In fact, we had to use four independent vibrational origins for the torsional components, see Table 1. The values determined for these four vibrational origins in ν_2 agree with their displacements predicted for the interaction with the torsional manifold correlating with $6\nu_4$, as shown in Fig. 8.

The anomalous torsional pattern in ν_2 is generated by the same mechanism causing a similar effect in ν_3, and explained by Bermejo et al. [13]. The mechanism involves the linear dependence of the torsional barrier parameter V_3 on the normal coordinate q_2.

Using a simple approximation, we write the torsional Hamiltonian as

$$\boldsymbol{H}_{\text{tors.}} = \boldsymbol{H}_0 + \boldsymbol{H}' \tag{7}$$

with

$$\boldsymbol{H}_0 = A\mathbf{J}_\tau^2 + \frac{1}{2}V_3^0(\cos 3\tau + 1) + \frac{1}{2}V_6(\cos 6\tau - 1) \tag{8}$$

and

$$\boldsymbol{H}' = \left(\frac{\partial V_3}{\partial q_2}\right)_0 \mathbf{q}_2(\cos 3\tau + 1) \tag{9}$$

assuming that the torsional angle τ is zero in the conformation of maximum energy (eclipsed).

A term (9) is allowed by symmetry for each totally symmetric normal coordinate (A_{1s} symmetry under the extended molecular group $G_{36}(EM)$, that is q_1, q_2 and q_3). The anomalous torsional pattern in ν_2 is caused by the term (9), therefore we tried to determine the value of the barrier derivative $\left(\frac{\partial V_3}{\partial q_2}\right)_0$. Starting with a free internal rotor basis, we calculated the torsional eigenfunctions of $\boldsymbol{H}_0$, for ν_4 up to 8, with A=2.674677 cm^{-1}, V_3 =1013.28 cm^{-1} and V_6 =8.798 cm^{-1}. Using the eigenvectors, we also calculated the matrix elements of $(\cos 3\tau+1)$, needed in the final calculation, in the basis of the eigenfunctions of $\boldsymbol{H}_0$. Then we built up the final matrix, on the basis of the functions $(v_2=0,v_4,\Gamma_t)$, $(v_2=1,v_4,\Gamma_t)$ and $(v_2=2,v_4,\Gamma_t)$, with v_4 varying from 0 to 8.

We assumed that the eigenvectors of these basis functions, in terms of the free internal rotor functions, were independent of the value of v_2. The matrix factors into four blocks, corresponding to the different symmetry species Γ_t, that is E_{3s}, E_{3d}, A_{1s} or A_{1d}, and A_{3d} or A_{3s} (A_{1s} and A_{3d} occur for even v_4 and A_{1d} and A_{3s} occur for odd v_4). Owing to the operator $\mathbf{q}_2$ and its selection rules, the matrix elements of $\boldsymbol{H}'$ link the functions with v_2=1 to those with v_2=0 and v_2=2. They contain the value of the derivative $\left(\frac{\partial V_3}{\partial q_2}\right)_0$, to be determined. The vibrational origins, $\nu_2(\Gamma_t) - \nu_4(\Gamma_t \times A_{3s})$, were calculated by diagonalization of the four matrix blocs, as eigenvalue differences $E(v_2=1,v_4=0,\Gamma_t)$ - $E(v_2=0,v_4=1,\Gamma_t\times A_{3s})$. They were compared to the values determined from the analysis of the spectrum, and the value of the derivative $\left(\frac{\partial V_3}{\partial q_2}\right)_0$ was iteratively adjusted by the least squares procedure.

Using a dimensionless normal coordinate q_2, we eventually found $\left(\frac{\partial V_3}{\partial q_2}\right)_0 = 127\pm10$ cm^{-1}, the large uncertainty being mostly related to the approximations involved in the calculations.

This value is considerably smaller (in the absolute value) than the barrier derivative with respect to q_3 determined by Bermejo et al. [13], -276 cm^{-1}, in agreement with the theoretical predictions of Kirtman et al. [14]. We note that the relative shifts of the four components of ν_2 are actually determined by the interaction with the manifold $6\nu_4$ shown in Fig. 7, owing to the resonance conditions. However a considerable global shift toward the low energy is caused by the interaction with the levels (v_2=2,v_4=0, Γ_t), because of the large matrix elements.

6. "Hot" difference bands: (ν_4+ν_{11}) – 2ν_4.

We could identify transitions from $2\nu_4$ to $\nu_4+\nu_{11}$, with $K''\Delta K$ from -2 to 9. The bias of this range, in favour of the positive values, is due to the fact that the origin of the band $(\nu_4+\nu_{11})-2\nu_4$ is higher than that of $\nu_{11}-\nu_4$ by about 34 cm^{-1}. Therefore the sub-branches of this "hot" difference band with positive values of $K''\Delta K$ move to the high wavenumbers, far from the center of $\nu_{11}-\nu_4$, as K'' increases. On the contrary, the sub-branches with negative $K''\Delta K$ move to the crowded center of the stronger $\nu_{11}-\nu_4$, and become hardly detectable. The line assignment, very difficult at the beginning, became easier when the values of the lower state J-structure parameters could be guessed from the line assignments already acquired.

In Table 2 we report the values of the rotational constants for the different torsional components of the $2\nu_4$ state, eventually determined from the differences of the observed wavenumbers of transitions sharing the same rotation-torsion level of $\nu_4+\nu_{11}$. Pairs whose calculated and observed differences deviated by more than 0.001 cm^{-1} were disregarded.

We also calculated values of B, D_J and D_{JK} assuming that they were equal in all torsional components. They are reported in the last column of Table 2.

A simple explorative least squares fit calculation of the observed wavenumbers showed that the levels of the stronger torsional component of the $\nu_4+\nu_{11}$ state with $k= \pm 2$, $l= \pm 1$ are heavily perturbed. Even excluding transitions to these levels from the body of data, we could obtain a fit of the observed data with a RMS deviation of 0.028 cm^{-1}, showing that a rather sophisticated model would be needed to try to analyze this state. We believe that the $(\nu_4+\nu_{11})-2\nu_4$ system would be conveniently analyzed together with the $\nu_4+\nu_{11}$ combination transition, having a common vibrational upper state. The latter has been studied by Susskind [7], but under the resolution of a grating spectrometer.

7. Conclusions.

Although the ν_{11} and ν_2 fundamentals of C_2H_6 are infrared inactive, a high resolution rotation-torsion analysis of these vibrational states has been performed through the investigation of the relative difference bands from the ν_4 torsional state. The detailed knowledge of these states can be relevant also in the applied research, because they can occur in infrared active combinations perturbing the absorption regions of atmospheric and planetary interest. In particular, the detailed knowledge of the infrared inactive ν_{11} and ν_2, together with the corresponding active modes ν_8 and ν_6, can be useful for the study of the 7 micron spectral region of $^{13}C^{12}CH_6$, expected to be quite similar to that of the main 12,12 isotopomer, but with all these four fundamentals active, because of the lowered symmetry.

The observation of the "hot" difference $(\nu_4+\nu_{11})-2\nu_4$ provides informations both on the lower state $2\nu_4$ and on the upper state $\nu_4+\nu_{11}$.

References

[1] J.R. Cooper, N. Moazzen-Ahmadi, J. Mol. Spectrosc. 239 (2006) 51-58.

[2] F. Lattanzi, C. di Lauro, J. Vander Auwera, Mol. Phys. in press,

[3] C. di Lauro, F. Lattanzi, J. Vander Auwera, J. Mol. Spectrosc. 267 (2011) 71-79.

[4] T. Ahonen, S. Alanko, V.-M. Horneman, M. Koivusaari, R. Paso, A.-M. Tolonen, and R. Anttila, J. Mol. Spectrosc. **181** (1997) 279 – 286.

[5] V.-M. Horneman, J. Opt. Soc. Am. B 21 (2004) 1050-1064.

[6] P.R. Bunker, P. Jensen, Molecular Symmetry and Spectroscopy, Second ed., NRC ResearchPress, Ottawa, 1998.

[7] J. Susskind, J. Mol. Spectrosc. 49 (1974) 1-17.

[8] J. T. Hougen, J. Mol. Spectrosc. 82 (1980) 92-116.

[9] C. di Lauro, F. Lattanzi, A. Valentin, Mol. Phys. 89 (1996) 663-676

[10] C. di Lauro, I.M. Mills, J. Mol. Spectrosc. 21 (1966) 386-413.

[11] C. di Lauro, F. Lattanzi, Mol. Phys. 103 (2005) 697-708.

[12] J.M. Fernández-Sánchez, S. Montero, J. Chem. Phys. 118 (2003) 2657-2672.

[13] D. Bermejo, J. Santos, P. Cancio, J.M. Fernández-Sánchez, S. Montero, J. Chem. Phys. 97 (1992) 7055-7063.

[14] B. Kirtman, W.E. Palke, C S. Ewig, J. Chem. Phys. 64 (1976) 1883-1890.

Legends of Tables

Table 1

Vibration-rotation-torsion parameters in cm^{-1} determined for the vibrational states ν_{11}, ν_2 and $\nu_3+2\nu_4$. Numbers in parentheses are standard deviations in units of the last quoted digit.

Table 2

Values in cm^{-1} of the rotational constants B, D_J and D_{JK} determined for the torsional components of $2\nu_4$, See text.

Table 1

	ν_{11}	ν_2	$\nu_3+2\nu_4$	ν_4
$\nu°$	1467.99167 (22)		1541.403 (690)	289 [a]
X	0.00110 (5)		1.2530 (585)	0.07870 [a]
$\nu°(A_{1s})$		1396.53269 (710)		
$\nu°(E_{3s})$		1396.51036 (791)		
$\nu°(E_{3d})$		1396.54163 (751)		
$\nu°(A_{3d})$		1396.51334 (820)		
A	2.6594550 (515)	2.6756371 (827)	2.64684 (506)	2.669693 [b]
B	0.66451488 (126)	0.6612137 (115)	0.652705 (236)	0.6604969 [b]
$10^5\times D_J$	0.106149 (199)	0.104302 (762)	0.103174 [c]	0.10231 [b]
$10^5\times D_{JK}$	0.23273 (100)	0.25602 (651)	0.26604 [c]	0.2726 [b]
$10^5\times D_K$	0.89205 (233)	0.9178 (243)	0.885 [c]	0.885 [b]
$A\bar{\zeta}$	-0.8956103 (198)			
$10^6\times\eta_J$	0.691 (102)			
$10^4\times\eta_K$	-0.50880 (279)			
$10^3\times F$	0.203976 (366)			
$10^5\times F_K$	0.1081 (98)			
$10^2\times E$	0.173046 (633)			
$10^6\times E_K$	-0.4134 (359)			

$Z_{2,11} = 0.3320924\ (309)$, $10^5\times Z_{J2,11} = -0.2186\ (99)$, $Z_{344,11} = 0.011287\ (121)$

[a] Assumed

[b] Ref. [2]

[c] As in the vibrational ground state, Ref. [2]

Table 2

	A_{1s}	E_{3d}	E_{3s}	A_{3d}	All
n. data [a]	14	47	58	44	77
$K''\Delta K$	6	1, 3, 5, 7	-2, 2, 4, 8	-3, 1, 3, 9	-3 to 9
J_{max}	20	19	22	21	22
B	0.65810	0.658106	0.658187	0.658225	0.658179
$10^5 \times D_J$	0.1364	0.1021	0.1019	0.1010	0.1006
$10^5 \times D_{JK}$		0.2651	0.2770	0.2784	0.3050

[a] number of combination differences used in the calculation.

Legends of Figures

Fig. 1

$^{r}Q_3$ sub-branch of ν_{11}-ν_4, showing the *J*-structure and the splitting into the two components with torsional symmetries A_{1d} (stronger) and E_{3d} (weaker) in the lower state. Transmittance in arbitrary units is reported on the ordinates.

Fig. 2

Component of torsional symmetry A_{3d} in the lower state (stronger torsional component) of the $^{r}Q_3$ sub-branch of (ν_4+ν_{11})-2ν_4. The weaker torsional component, E_{3d}, occurs about 4 cm^{-1} at the higher wavenumbers.

Fig. 3

Coriolis interactions about the x,y axes of ν_{11} with the parallel vibrational states ν_2 and ν_3+2ν_4, shown as solid lines connecting interacting pairs of levels. Resonance occurs at *K* between 12 and 13 in ν_2 (with the (-*l*)-side of ν_{11}) and between 11 and 12 in ν_3+2ν_4 (with the (+*l*)-side of ν_{11}). Dotted lines connect pairs of levels of ν_{11} interacting by *l*(2,-1) coupling, with Δl=±2 and $\Delta k = \mp 1$. The energy levels have been calculated for *J*=15 at several values ±*K*, with disregard of these Coriolis interactions (zero-order energies).

Fig. 4

P-transitions from ν_4 to ν_2 with torsional splitting, identified as K_J (quantum numbers of the lower state), for K=11, 12, 13. They are made observable by intensity stealing from the stronger transitions from ν_4 to ν_{11}, in the region of near Coriolis resonance of ν_2 and ν_{11}. See text.

Fig. 5

l-type interactions in the ν_{11} vibrational state of ethane. The *l*(2,2) interaction causes the splitting of the *l*=*k*=±1 pair, which is transmitted to the $l = \mp 1$, *k*=±2 pair by the *l*(2,-1) coupling, see text.

Fig. 6

$^{p}Q_3$ sub-branch, showing the effects of torsional and K-splitting. The split K_+ and K_- components are defined according to Equation (6), applied to the upper state wavefunctions, see text and Fig. 5. The torsional splitting (A_{1d} and E_{3d} components in the lower state) is almost constant, whereas the K-splitting increases with the total angular momentum quantum number *J*. The K+ and K- components show opposite intensity alternations with the parity of *J*, the former being stronger at the odd values and the latter at the even values. Note the small separation of the lines with *J* equal to 14 and 15 in K+, and the inversion of the relative positions of K+ and K- starting at *J*=15. See text, and Fig. 5 and 6.

Fig. 7

$^{r}Q_0$ sub-branch of ν_{11}-ν_4, showing the torsional splitting (A_{3s} and E_{3s} torsional symmetries in the lower state) and the typical intensity alternation with the parity of *J*. These transitions occur to the components – of the *l*-doublets with $k = l = \pm 1$. Note the large separation between the lines with *J* equal to 14 and 15, caused by the *J*-crossing in a *l*(2,-1) resonance, and the s-type transitions (ΔK=2), marked by a prime, activated by this resonance at *J*= 14 and 15. See text and Fig. 5 and 7.

Fig. 8

Splitting induced in the ν_2 state by the interaction with the nominal $6\nu_4$ state, exhibiting large torsional splittings. The interaction matrix elements are represented by dotted lines, and the relative displacements induced on the torsional components of ν_2 (much exaggerated) are qualitatively represented by arrowed lines. The pattern of the torsional components of ν_2, in the order of increasing energies, becomes E_{3s}, A_{3d}, A_{1s}, E_{3d}. See text.

Fig. 1

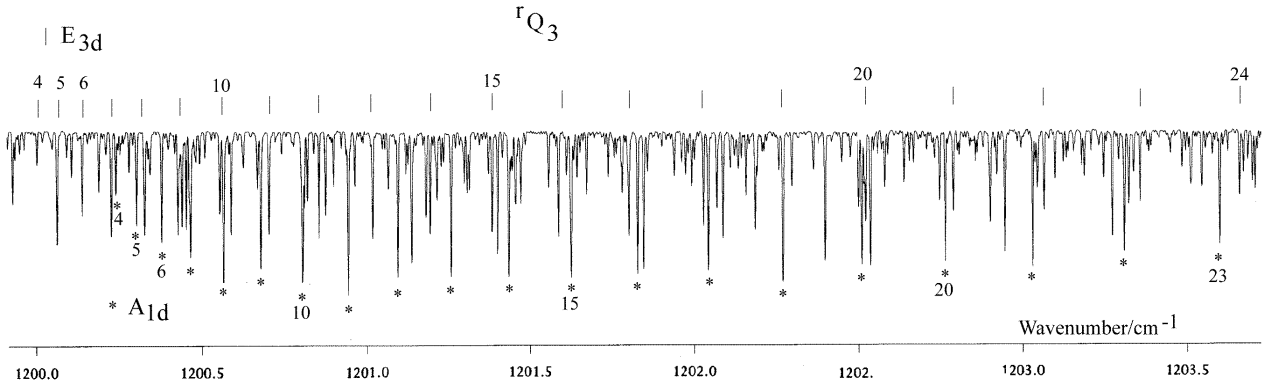
E 3d
r Q 3
4 5 6
10
15
20
24
A 1d
Wavenumber/cm -1
1200.0
1200.5
1201.0
1201.5
1202.0
1202.
1203.0
1203.5

Fig. 2

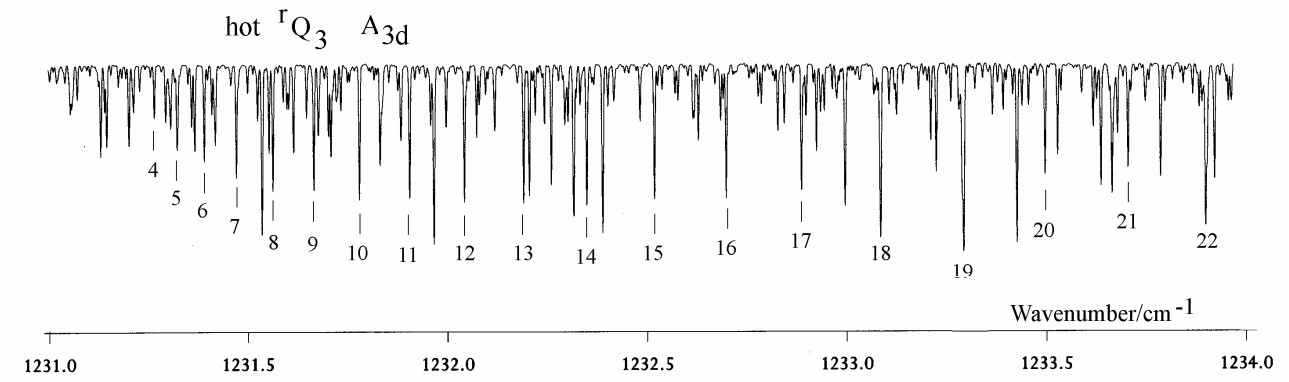
hot r Q 3
A 3d
4 5 6 7 8 9 10 11 12 13 14 15 16 17 18 19 20 21 22
Wavenumber/cm -1
1231.0
1231.5
1232.0
1232.5
1233.0
1233.5
1234.0

Fig. 3

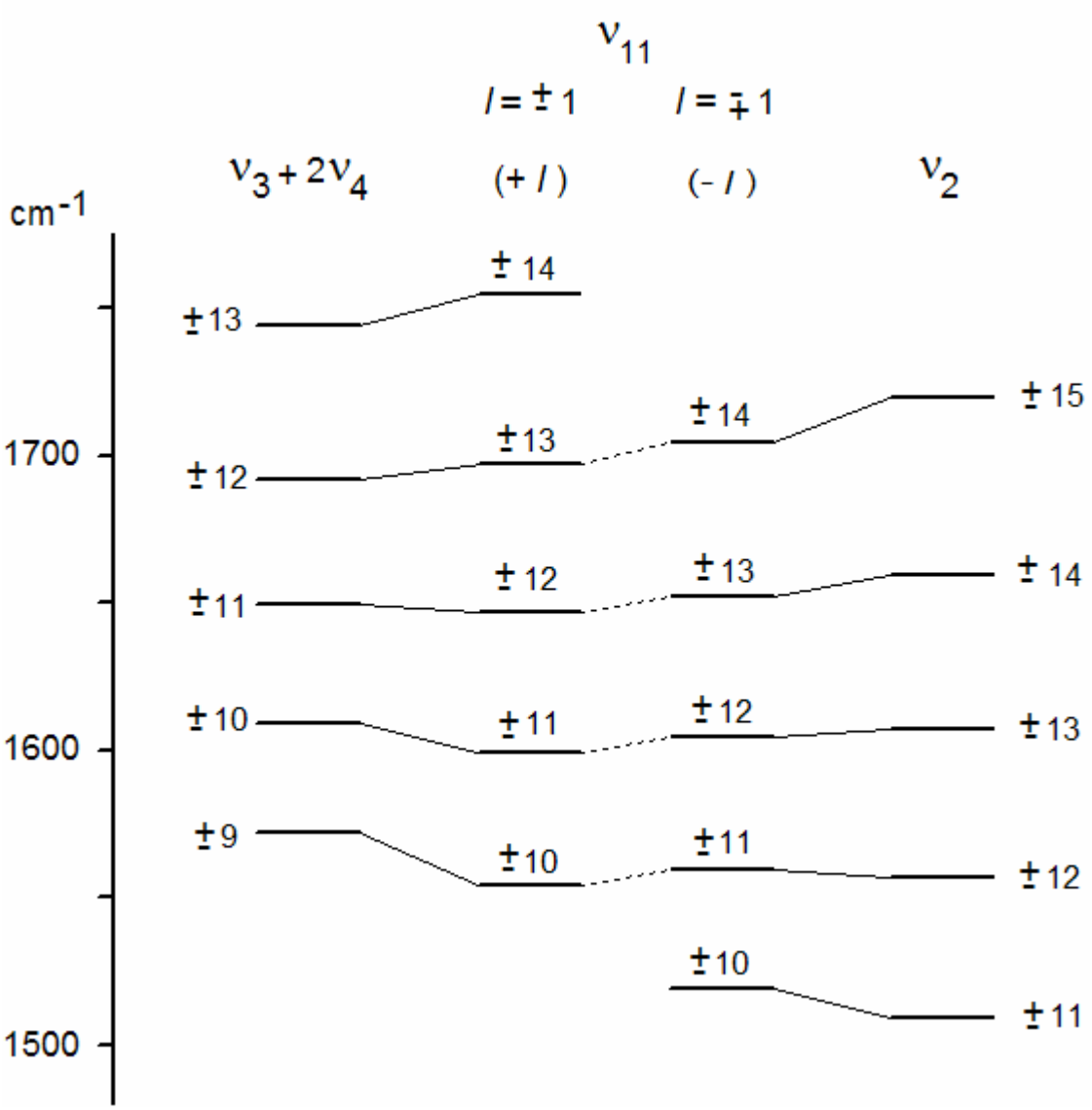
ν11
l = ± 1
l = ∓ 1
ν3 + 2ν4
(+ l)
(- l)
ν2
cm-1
1700
1600
1500
± 14
± 13
± 15
± 13
± 14
± 12
± 12
± 13
± 14
± 11
± 11
± 12
± 13
± 10
± 10
± 11
± 12
± 9
± 10
± 11
± 12
± 10
± 11

Fig. 4

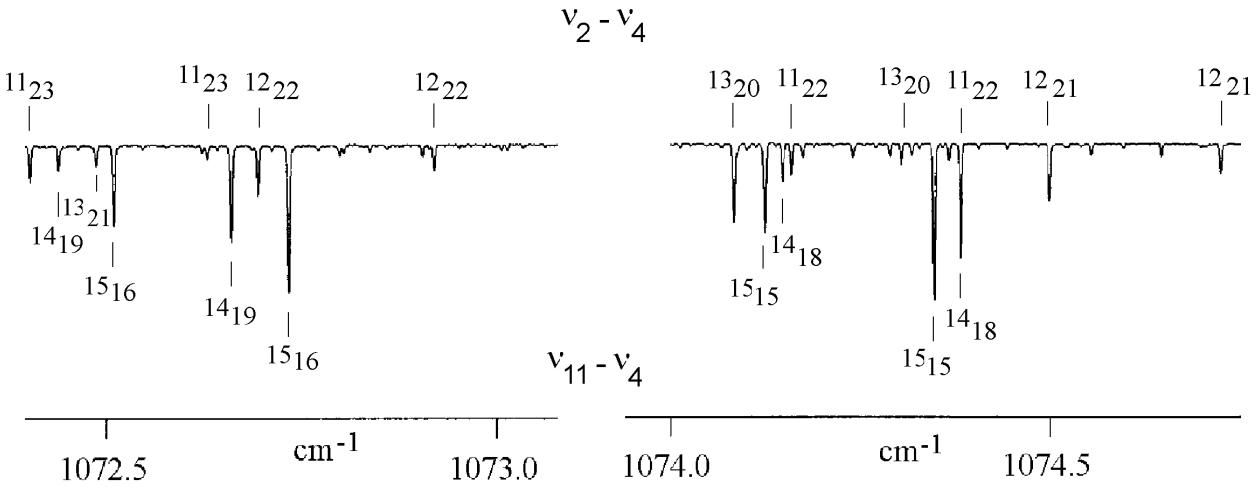

Fig. 5

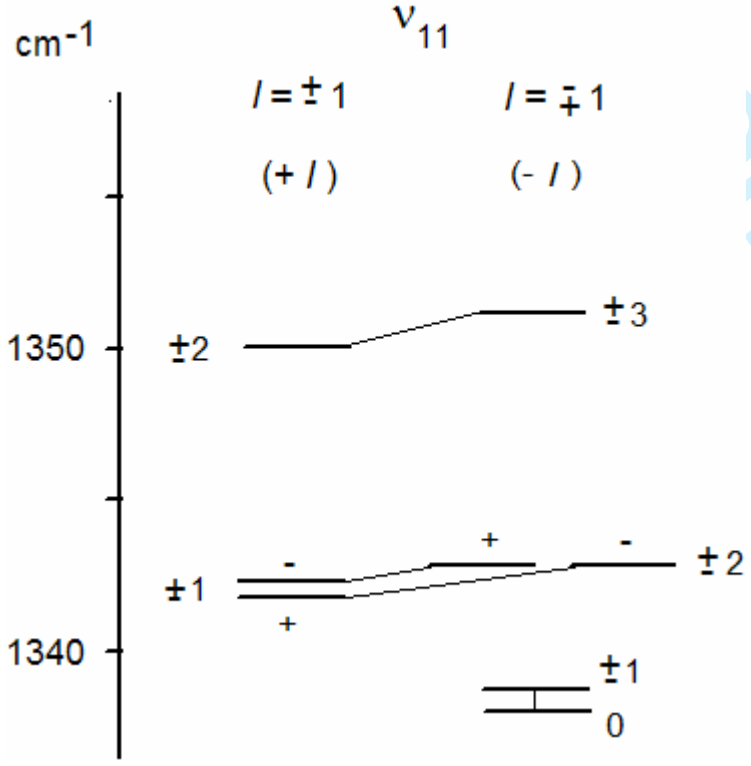

Fig. 6

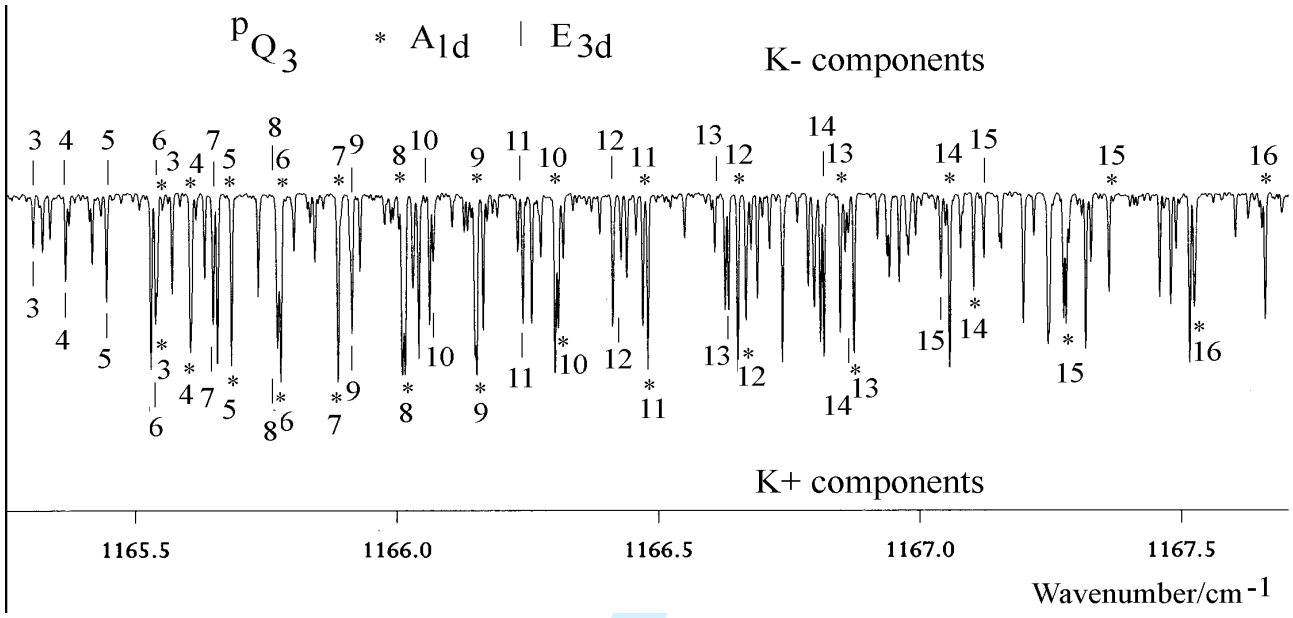

Fig. 7

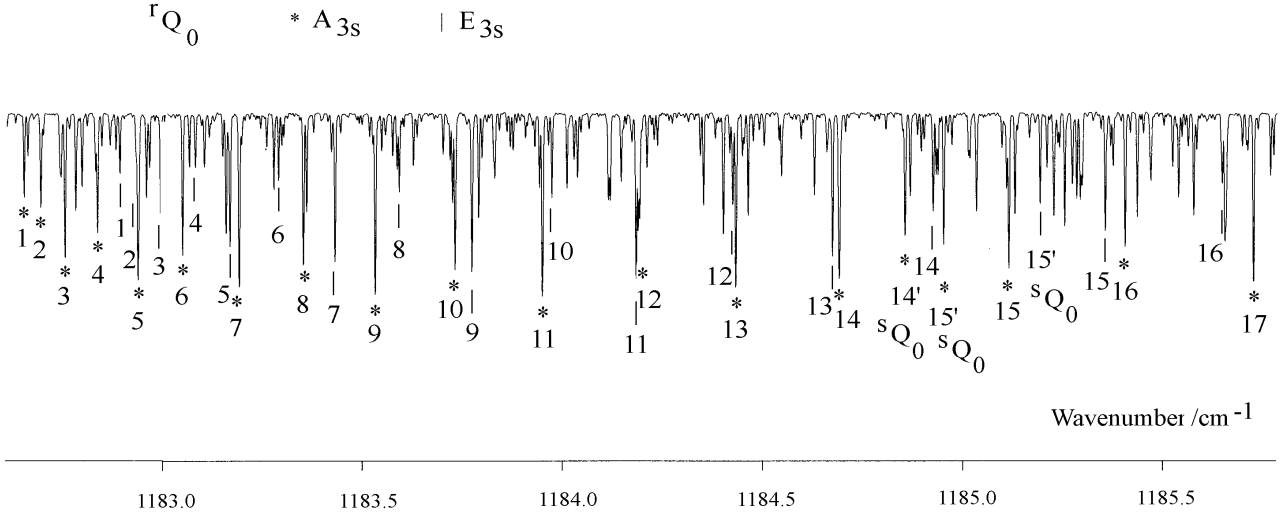

Fig. 8